

Epigallocatechin-3-Gallate Allosterically Activates Protein Kinase C- α and Improves the Cognition of Estrogen Deficiency Mice

Shuai Zhang, Yi Xu, Lu Zeng, Xiaobin An, Dan Su, Yang Qu, Jing Ma, Xin Tang, Xuqiao Wang, Junkai Yang, Chandan Mishra, Shah Ram Chandra, and Jing Ai*



Cite This: <https://doi.org/10.1021/acscchemneuro.1c00401>



Read Online

ACCESS |

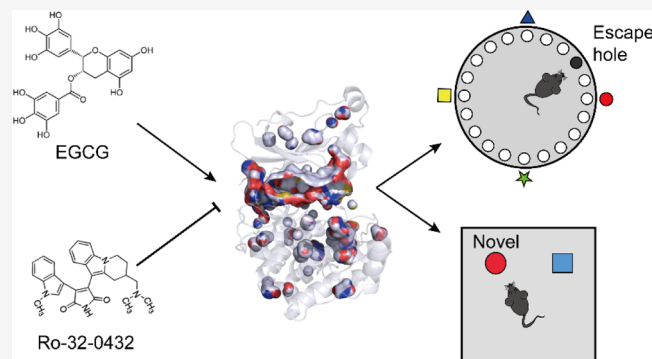
Metrics & More

Article Recommendations

Supporting Information

ABSTRACT: Protein kinase C (PKC) isoforms play essential roles in biological processes, and activation of PKC is proposed to alleviate the symptoms of a variety of diseases. It would be of great significance to find effective pharmacological modulators of PKC isoforms that can be translated for clinical use. Here, using *in vitro* activity assay, we demonstrated that green tea extract ($-$)-epigallocatechin-3-gallate (EGCG) dose-dependently activated PKC α with a half effective concentration (EC₅₀) of 0.49 μ M. We also performed surface plasmon resonance analysis and found that EGCG binds PKC α with an equilibrium dissociation constant (K_D) value of 4.11×10^{-6} mol/L. Further computational flexible docking analysis revealed that EGCG interacted with the catalytic C3–C4 domain of PKC α (PDB: 4RA4) through establishing polar hydrogen bonds with V420, T401, E387, and K368 of PKC α , and the benzene ring group of EGCG hydrophobically interacted with the hydrophobic pocket formed by L345, M470, I479, and V353 of PKC α . Interestingly, the PKC α -selective blocker Ro-32-0432 could compete with EGCG for the same substrate-binding pocket of PKC α . Moreover, we found that EGCG dose-dependently improved the spatial memory, object recognition ability, and hippocampal long-term potentiation of ovariectomized mice, which was offset by Ro-32-0432. Collectively, our findings reveal a novel PKC α agonist and open the way to a new perspective on PKC α pharmacology and the treatment of PKC α -related diseases, including cognitive impairment.

KEYWORDS: PKC α , EGCG, OVX, cognition, Ro-32-0432



INTRODUCTION

Protein kinase C (PKC) is a family of protein kinase enzymes that play essential roles in transmembrane signal conduction through phosphorylating the substrate proteins.¹ Evidence is emerging that PKC isoforms are critically involved in a variety of signal pathways regulating cell growth, differentiation, apoptosis, transformation, tumorigenicity, and synaptic function.² As such, PKC participates in many important human diseases, including heart disease,³ diabetes mellitus,⁴ tumorigenesis,⁵ and Alzheimer's disease (AD).⁶ Therefore, finding effective ways to modulate the PKC function would be of great significance for the treatment of PKC dysfunction-induced diseases.

Based on the second messenger requirements, PKC isoforms can be classified into the conventional, novel, and atypical PKC.⁷ Among these isoforms, conventional PKC α is widely expressed in all tissues, particularly prominent in the brain,⁸ which increases the difficulty of intervention because of its general function. Previous *in vivo* studies have already revealed the extensive action of PKC α activation. In the cardiovascular system, PKC α activates eNOS and increases arterial blood flow *in vivo*,⁹ while PKC α deletion causes

hypotension and decreased vascular contractility.¹⁰ In the renal system, PKC α activation promotes recovery of mitochondrial function and cell survival following oxidant injury in renal cells.¹¹ Besides, activation of PKC α prevents the synaptic loss, A β elevation, and cognitive deficits in AD transgenic mice.^{12,13} However, PKC α activation cannot always induce positive effects. All PKC activators downregulate PKC at high concentration or long application duration.¹⁴ Bryostatin-1, a widely used high-affinity (1.35 nM) PKC activator in basic research, activates PKC α by hydrogen bonds to Gly253, Thr242, and Leu251, while produces a prolonged down-regulation.^{15–17} In phase II clinical studies, bryostatin-1 has minimal to no benefit in various cancers and causes severe myalgias in >50% of patients.^{18,19} What is worse, some other PKC activators, such as phorbol 12-myristate 13-acetate which

Received: June 16, 2021

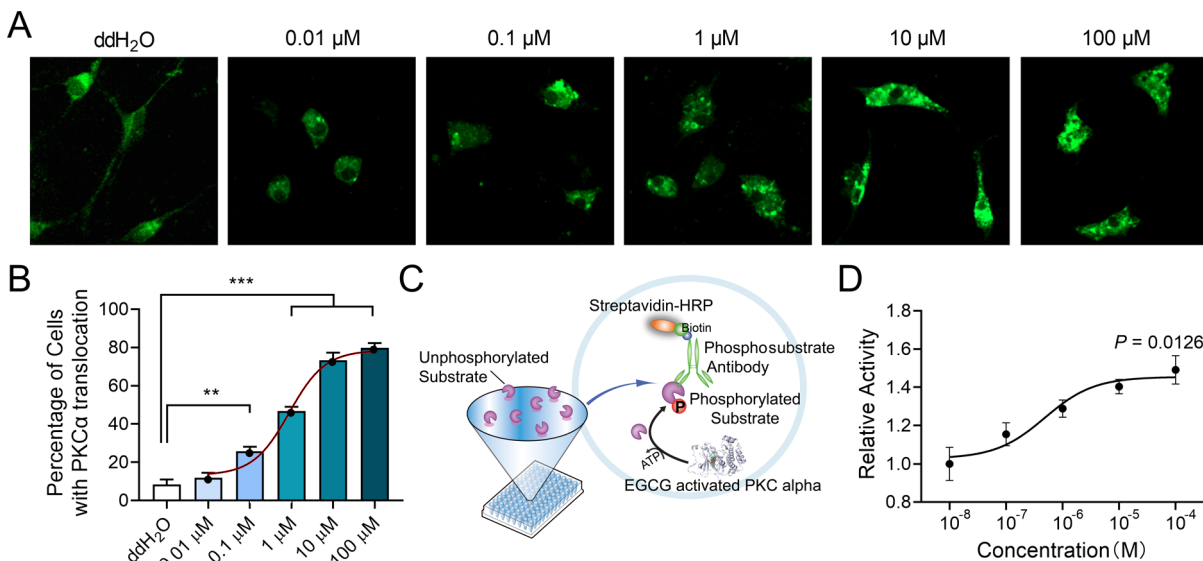


Figure 1. EGCG allosterically activates PKC α *in vitro*. (A) Primary cultured neurons transfected with PKC α -GFP were treated with EGCG at 10^{-8} to 10^{-4} mol/L for 60 min, respectively. (B) Percentage of cells displaying EGCG-induced subcellular redistribution of PKC α . The fitted red curve shows the activation curve of EGCG on PKC α ($n = 3$ batches of cells for each group). (C) Procedure of the ELISA experiment. Unphosphorylated substrates were attached to the ELISA plate. EGCG and PKC α co-incubated for 1 h and then added into the reaction hole. Phosphorylated substrate antibody was used to bind the phosphorylated substrate, and streptavidin-HRP was used to label the substrate-bind antibody. (D) Activation curve of PKC α by EGCG. EGCG dose-dependently activates PKC α , 10^{-4} mol/L EGCG activates 1.5-fold PKC α compared to 10^{-8} mol/L EGCG.

is a kind of phorbol ester competing with the DAG-binding site of PKC, are potent tumor promoters.²⁰ Therefore, a novel nontumorigenic and cost-effective mild PKC α activator will offer therapeutic benefits for PKC α -related diseases.

Diet-derived compounds are generally regarded as safe based on their long history of use in the diet or as traditional medicines.²¹ Given the concerns about this, we searched for an activator of PKC α from food-derived natural compounds and focused on (−)-epigallocatechin-3-gallate (EGCG, (2R,3R)-2-(3,4,5-Trihydroxyphenyl)-3,4-dihydro-1(2H)-benzopyran-3,5,7-triol 3-(3,4,5-trihydroxybenzoate)), the major form of catechins from green tea.²² Previous *in vivo* studies showed that EGCG has strong anti-tumor, anti-inflammatory, and anti-oxidative effects.²³ Importantly, it is also a neuroprotective agent, which promotes the phosphorylation of PKC and relieves A β toxicity.^{24–27} However, these findings provide no insights into whether EGCG can allosterically modulate PKC α activity, a question we investigate in the present study.

In the present study, combining molecular biological and chemical methods, we identified the activator property of EGCG on PKC α . Using electrophysiological and behavioral experiments, we observed that *in vivo* administration of EGCG could rescue the cognitive impairment of estrogen-deficient mice through activating PKC α . Importantly, EGCG may also represent a valuable therapeutic alternative in other pathologies involving impairments of the PKC α -signaling pathway.

RESULTS AND DISCUSSION

EGCG Allosterically Activates PKC α In Vitro. The translocation of PKC from the cytosol to either the plasma membrane or internal membranes is a well-known hallmark of PKC activation.^{7,28} Therefore, to assess the PKC α activator potential of EGCG *in vitro*, we constructed a GFP-fused PKC α plasmid and administrated 0.01–100 μ M EGCG to the PKC α -GFP transfected primary cultured neurons. One hour later, we

found that EGCG dose-dependently triggered the formation of dense immunofluorescent PKC α particles in neurons (Figure 1A,B), which is considered the sign of subcellular redistribution.²⁹ Dose-dependent analysis of PKC α translocation in neurons revealed an EC₅₀ (concentration required to induce a 50% effect) value of 0.91 μ M. However, this cell treatment experiment could not confirm whether EGCG activated PKC α through direct interaction or not. To this issue, we performed an *in vitro* kinase activity assay using recombinant human PKC α . In this assay, 10^{-8} to 10^{-4} M EGCG were allowed to incubate and directly interact with PKC α , the activated PKC α then phosphorylated the substrates whose phosphorylated form could be detected by a biotin-labeled antibody (Figure 1C). Consequently, we found that EGCG dose-dependently activated PKC α with an EC₅₀ value of 0.49 μ M (Figure 1D). Altogether, these results strongly indicated that EGCG allosterically activates PKC α .

EGCG Binds PKC α through Interacting with the Catalytic C3–C4 Domain. To further clarify the binding affinity between EGCG and PKC α , we next performed a surface plasmon resonance (SPR) analysis. For the determination, His-tagged full-length PKC α was immobilized on the sensor chip, and EGCG at a series of concentrations (0–100 μ M) was set as mobile phase (Figure 2A). The binding manner was processed following the application of EGCG and kinetically analyzed using a 1:1 L interaction model. As demonstrated in Figure 2B and Table S1, EGCG established moderate intensity interaction with PKC α with a K_D value of 4.11×10^{-6} mol/L.

We then would like to predict the potential binding conformation between EGCG (Figure 2C) and PKC α . Due to the lack of intact PKC α crystal structure, we screened the C1 domain (PDB: 2ELI) (Figure S1A), C2 domain (PDB: 4DNL) (Figure S1B), and catalytic C3–C4 domain (PDB: 4RA4) (Figure S1C) of the PKC α structure with Pymol, and

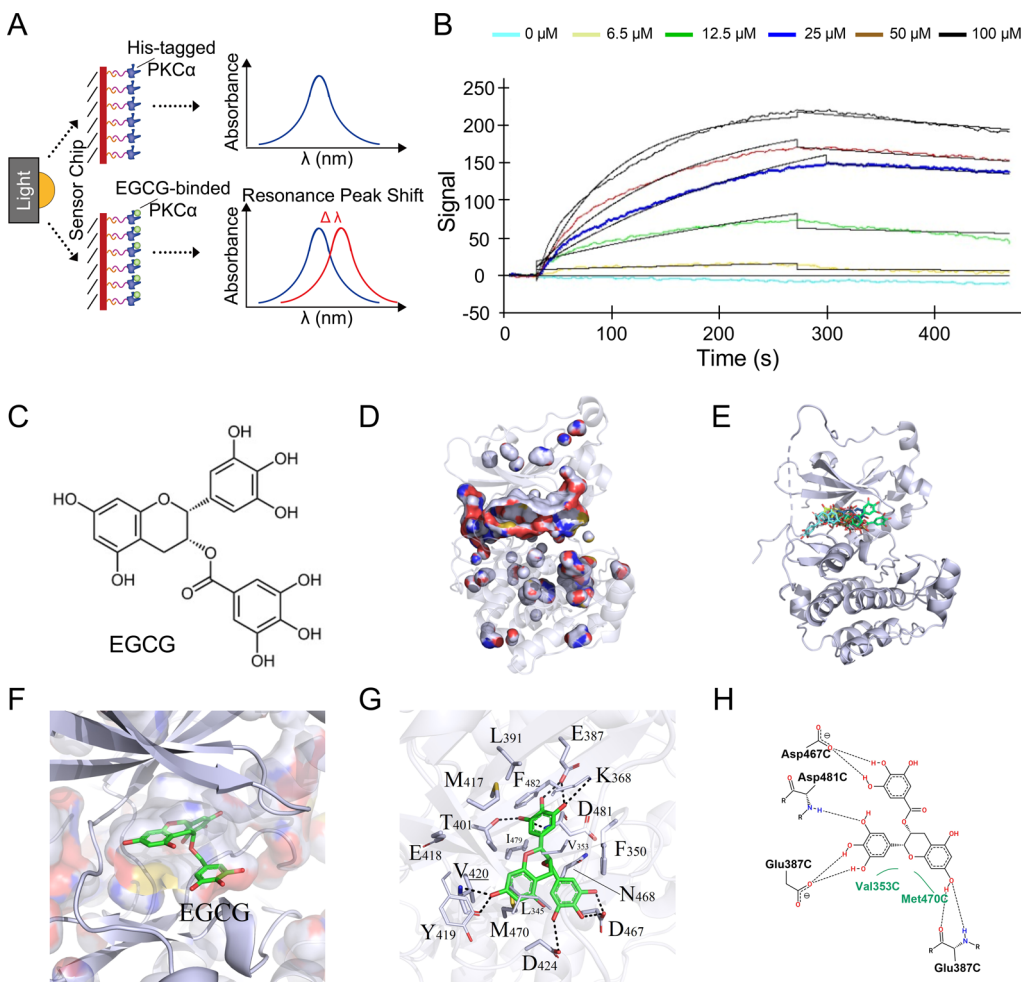


Figure 2. Molecular docking studies for EGCG interaction with PKC α . (A) Procedure of SPR analysis-localized SPR, His-tagged PKC α was attached on the sensor chip, and the mobile phase was ddH₂O or EGCG solution. The binding of EGCG to PKC α leads to a resonance peak shift. (B) Binding curves of serial concentrations of EGCG on the PKC α sensor chip by SPR. (C) Chemical structure of EGCG. (D–H) Molecular docking prediction of EGCG on PKC α . (D) PyMOL predicted active pocket of PKC α . (E) Predicted binding mode between 30 EGCG molecules with the active pocket of PKC α . (F) Pose view of the interaction of EGCG with PKC α with the lowest binding energy. (G) Top-ranked docking conformation of EGCG with K368, E387, T401, V420, D424, and D467. The hydrogen bonds between EGCG and these residues are also displayed through a dotted black line. (H) 2D diagrams of the interactions of PKC α with EGCG.

identified an active substrate-binding pocket on the catalytic C3–C4 domain of PKC α (Figure 2D). Subsequently, 30 docking conformations between EGCG and PKC α were predicted through a flexible docking algorithm with AutoDock 4.2 (Figure 2E, and detailed in Table S2). Among 30 docking conformations, the lowest binding energy was -10.16 kcal/mol (Figure 2F and Table S2), and this conformation was then extracted for further molecular dynamics analysis. The entire protein system uses gaff and ff14SB force fields, with the protein as the center. The topological and coordinate structure was saved after adding a 10 Å cubic water box and Na⁺. As shown in Figure 2G,H, in the substrate-binding pocket, the phenolic hydroxyl groups of EGCG establish direct hydrogen bonds with V420, T401, E387, and K368 of PKC α . Besides, the benzene ring group of EGCG hydrophobically interacts with the hydrophobic pocket formed by L345, M470, I479, and V353 of the protein. The hydroxyl group inserts into the hydrophobic pocket, which enhances the polar interaction. To resolve the crystal structure of the EGCG-binding motif, we extract a 135 amino acid protein sequence from PKC α based on the molecular docking analysis. The amino acid sequence

is: LGKGSFGKVMLADRKGTEELYAIKILKKDVVIQ-DDDVECTMVEKRLALLDKPPFLTQLHSCFQTVD-RLYFVMEYVNGGDLMYHIQVQGVGFKEPQAVFYAAEISIGLFLHKRGIYRDLKLDNVMLDSEGHIKI. In this sequence, L1, V9, K24, E43, T57, V76, M126, and I135 are the key residuals for the binding of EGCG (Figure S2). The results provided evidence that EGCG could allosterically activate PKC α , acting at the catalytic C3–C4 domain.

PKC α -Selective Antagonist Ro32-0432 Competitively Blocks the Binding of EGCG with PKC α . For the further functional study, we looked for an antagonist to block the binding between EGCG and PKC α . Therefore, Ro-32-0432, a previously reported PKC α -selective antagonist, was selected (Figure 3A). Similar to EGCG, we first used AutoDock 4.2 to seek the Ro-32-0432-binding site on PKC α . Thirty docking poses were predicted through the flexible docking algorithm (Figure 3B), and the docking pose with the lowest binding energy (-12.54 kcal/mol) was then used for the following molecular dynamics analysis. As shown in Figure 3C,D, the carbonyl oxygen of Ro-32-0432 establishes direct polar hydrogen bond interaction with V420 of PKC α . Surprisingly,

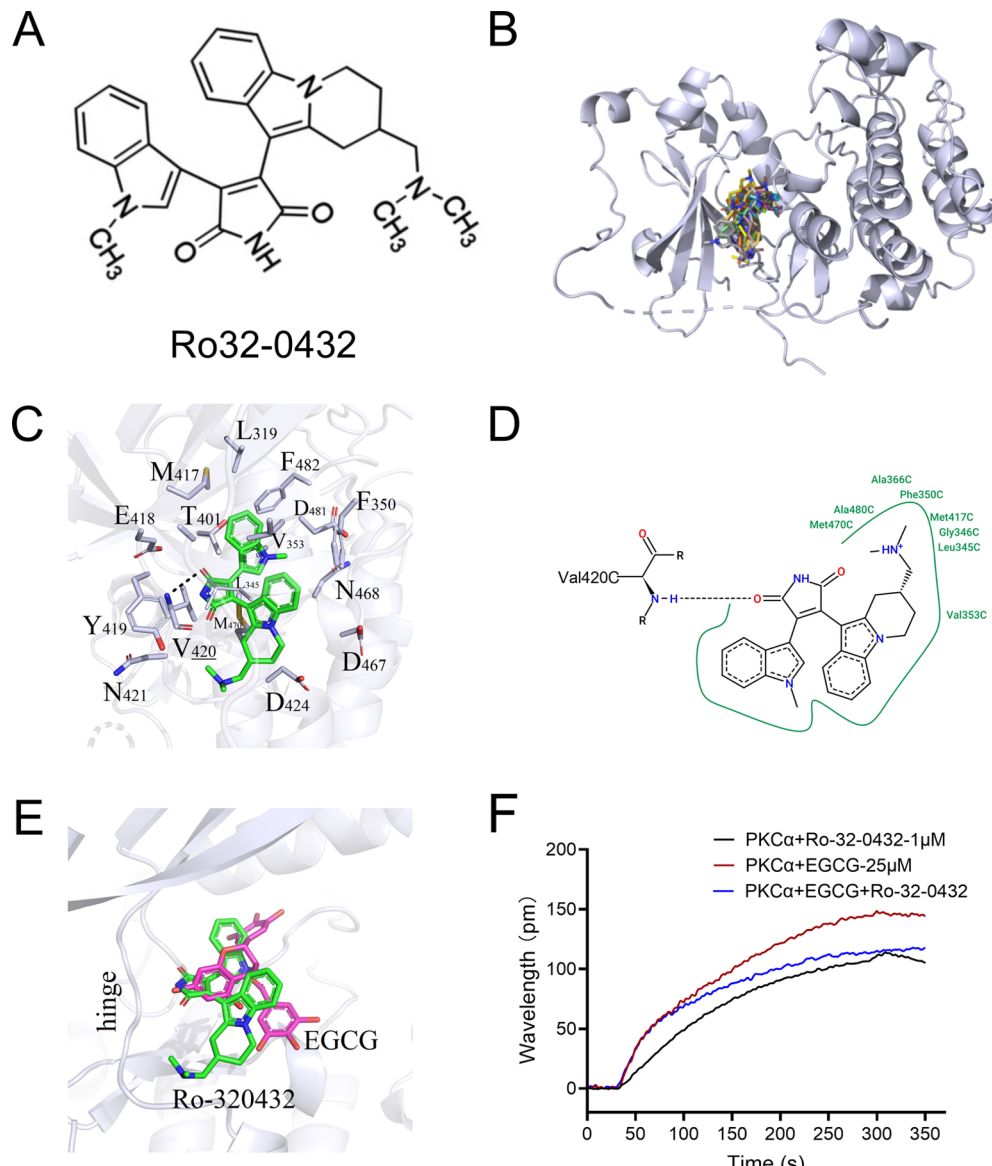


Figure 3. PKC α -selective antagonist Ro32-0432 competitively blocks the binding of EGCG with PKC α . (A) Chemical structure of Ro32-0432. (B–D) Molecular docking prediction of EGCG on PKC α . (B) Thirty predicted binding poses between Ro32-0432 molecules with the active pocket of PKC α . (C) Pose view of the interaction of Ro32-0432 with V420. The hydrogen bonds between Ro-32-0432 and these residues are also displayed through a dotted black line. (D) 2D diagrams of the interactions of PKC α with Ro32-0432. (E) Overlay of EGCG and Ro-32-0432 in the active pocket of PKC α . (F) Binding curves of 1 μ moL Ro-32-0432, 25 μ moL EGCG, or 1 μ moL + 25 μ moL EGCG on the PKC α sensor chip by the OpenSPR system.

the same with EGCG, the benzene ring group of Ro-32-0432 also hydrophobically interacts with the hydrophobic pocket formed by L345, M470, I479, and V353 of PKC α , and the hydroxyl group inserts into the hydrophobic pocket too. Thus, EGCG and Ro-32-0432 shared the same active pocket of PKC α . Ro-32-0432 competes for the substrate-binding pocket and forms a more stable conformation with lower binding energy than EGCG (Figure 3E). The next SPR analysis revealed that 1 μ moL Ro-32-0432 could already produce a strong PKC α -binding signal. When 1 μ moL Ro-32-0432 and 25 μ moL EGCG were mixed and set as the mobile phase, the whole system finally equilibrated with a resonance value as the peak PKC α -binding signal of Ro-32-0432 (Figure 3F). Collectively, these results suggested that Ro-32-0432 effectively blocked the binding of EGCG with PKC α competitively.

EGCG Rescues the Cognitive Impairment of OVX Mice by Activating PKC α . The specificity of EGCG to PKCs is determined by the amino acid sequence of PKCs. In the molecular docking analysis, we found that the binding of PKC α and EGCG was mainly determined by the amino acids from L345 to I479. Among these amino acids, L345, V353, K368, E387, T401, V420, M470, and I479 were predicted to directly interact with EGCG. However, a comparison of amino acid sequences of PKC isozymes shows that these key amino acids are only conservative in PKC α and PKC β (Table S3). Furthermore, PKC α concentrates in the hippocampus³⁰ and is reported to be uniquely responsible for integrating spatiotemporally distinct Ca^{2+} signals during facilitating synaptic plasticity.³¹ Therefore, we consider that PKC α is the major and key target of EGCG in the hippocampus. To further investigate whether EGCG could rescue the impaired cognitive

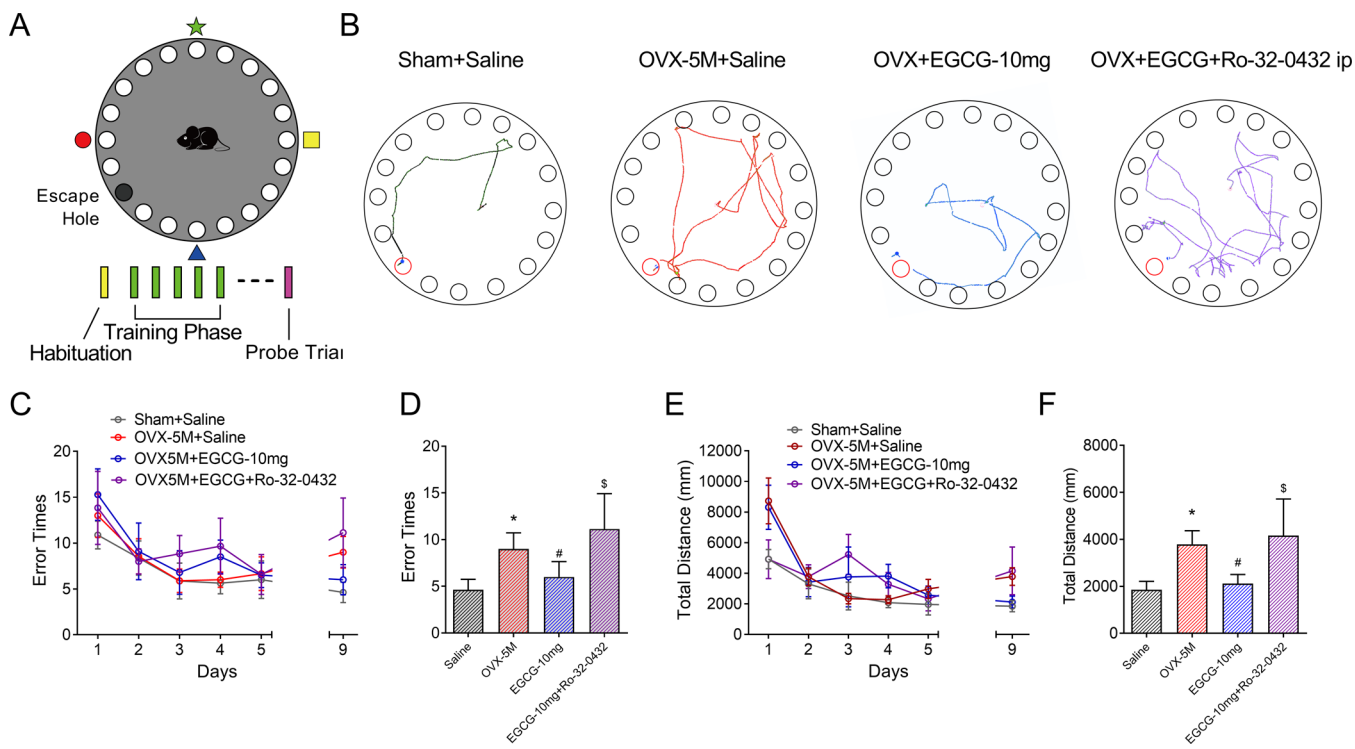


Figure 4. EGCG improves the spatial memory of OVX mice through activating PKC α . (A) Apparatus and procedure of the Barnes maze test. (B) Representative path tracings of the probe test on day 9 in the Barnes maze test for each group. (C) Mean daily error times to find the escape hole during the training and probe trials. (D) In the probe trial, compared with sham mice ($n = 8$), OVX-5M mice ($n = 9$) experience more error times to find the escape hole. EGCG decreases the error times of OVX mice [10 ($n = 9$) mg/kg/day]. Co-injection of Ro-32-0432 ($n = 7$) significantly increases the error time of 10 mg/kg/day EGCG-treated OVX mice. (E) Mean daily travel distance to find the escape hole during the training and probe trial. (F) In the probe trial, compared with sham mice, OVX-5M mice experience more travel distance to find the escape hole. EGCG decreases the travel distance of OVX mice. Co-injection of Ro-32-0432 significantly increases the travel distance of 10 mg/kg EGCG-treated OVX mice. Mean \pm SEM, * $P < 0.05$ vs Sham mice, # $P < 0.05$ vs OVX-5M mice, \$ $P < 0.05$ vs OVX-5M + EGCG (10 mg/kg/day) mice.

function by activating PKC α *in vivo*, we selected the estrogen deficiency-induced memory deficits mice model which was previously demonstrated with downregulated hippocampal PKC α .³² We intraperitoneally injected 5, 10, and 20 mg/kg/day EGCG to 4 month ovariectomized (OVX) mice. One month later, we assessed the spatial memory of EGCG-treated mice with Barnes maze (Figure 4A) and found that EGCG administration dose-dependently decreased the error times and travel distance of OVX mice to find the escape hole in the probe trial (Figures 3B–F, S3A–E). Importantly, to explore whether the *in vivo* neuroprotective effect of EGCG depends on PKC α , we intraperitoneally administrated Ro-32-0432 (50 μ g/kg/day)³³ simultaneously with 10 mg/kg/day EGCG to OVX mice. As expected, Ro-32-0432 totally blocked the improvement of spatial memory induced by EGCG (Figures 4B–F and S3A–E). Except for spatial memory, we also evaluated the episodic memory ability of mice with novel object recognition tests (Figure 5A). Compared with saline-treated OVX mice, we found that 10 or 20 mg/kg/day EGCG administration significantly increased the exploration duration on novel objects, while only 20 mg/kg/day EGCG administration increased the exploration frequency on novel objects. 5 mg/kg/day administration of EGCG could not rescue the object recognition memory of OVX mice (Figures 5B,C and S3F,G). Thus, the behavioral tests demonstrated that EGCG improved spatial and object recognition memory of OVX mice through activating PKC α .

Although no evidence shows the direct interaction between EGCG and PKC α , previous studies have reported the

increased phosphor-PKC α and ERK1/2 following EGCG administration.³⁴ Furthermore, PKC α is recently reported as the only PKC isozyme required for the facilitation of synaptic plasticity.³¹ Therefore, we evaluated the activation of PKC α with long-term potentiation (LTP), which is the basis of learning and memory.³⁵ After the behavioral tests, therefore, we recorded the hippocampal LTP of mice (Figures 5D and S4A). Consistent with the results of behavioral tests, we found that 5, 10, and 20 mg/day EGCG administration dose-dependently rescued the hippocampal LTP of OVX mice (Figure 5E,F). Bath application of Ro-32-0432 (20 nmol/L) reverted the rescued hippocampal LTP of EGCG treated OVX mice (Figure S4B,C). Furthermore, the intraperitoneal administration of Ro-32-0432 also blocked the enhancement of hippocampal LTP induced by EGCG (10 mg/day) (Figure 5E,F). Altogether, these results demonstrated that EGCG has high *in vivo* cognitive protection activity through activating PKC α .

The conventional PKC α , which plays essential roles in transmembrane signal conduction as other PKC isoforms, was reported downregulated in lots of pathological conditions, like tumor,³⁶ hepatic,³⁷ heart,³⁸ and central nervous system diseases.^{13,39} Considering the unacceptable side effects of previous agonists,¹⁴ we would like to search for a novel, safe, and cost-effective PKC α activator in the present study.

Catechins flavonoids are contained in green tea extract (GTE) and are defined as the active components of green tea, accounting for its therapeutic properties. EGCG represents the principal bioactive polyphenol in the solid GTE.⁴⁰ It has been

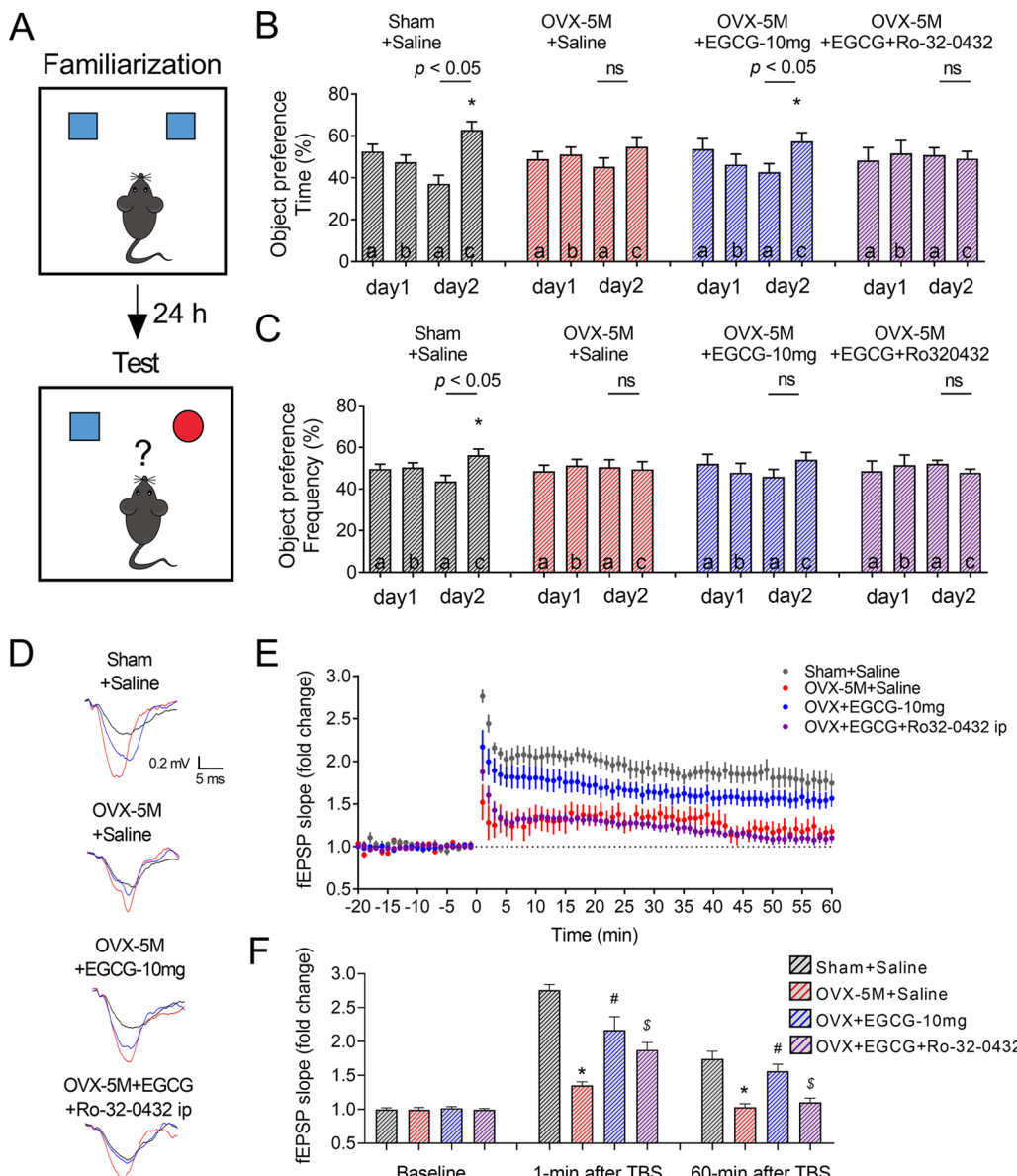


Figure 5. EGCG improves the object recognition memory and rescues the hippocampal LTP of OVX mice through activating PKC α . (A) Diagram of novel object recognition memory tasks. In the familiarization phase, two identical objects were placed in the apparatus. 24 h later, one of the objects was replaced by a new one. (B,C) Object preference (time and frequency) of Sham ($n = 8$) and OVX mice after intraperitoneal injection of saline, EGCG [10 mg/kg/day, ($n = 9$)], or EGCG (10 mg/kg/day) + Ro32-0432 (50 μ g/kg/day) ($n = 7$). * $p < 0.05$ vs the familiar object. (D) Representative fEPSP traces (black traces: baseline fEPSP and red and blue traces: fEPSP recorded 1 and 60 min after TBS) of the hippocampal CA3-CA1 pathway obtained at the times indicated by the numbers in the time-course graph on panels B and C. (E,F) Averaged time course and magnitude of LTP of Sham ($n = 8$), OVX-5M ($n = 10$), OVX-5M + EGCG [10 mg/kg/day ($n = 10$)], and OVX-5M + EGCG + i.p. administrated Ro-32-0432 ($n = 9$) mice. (F) Summary of the changes in the hippocampal fEPSP slopes of the abovementioned mice after 1 and 60 min of TBS. Mean \pm SEM, * $P < 0.05$ vs Sham mice, # $P < 0.05$ vs OVX-5M mice, \$ $P < 0.05$ vs OVX-5M + EGCG (10 mg/kg/day) mice.

reported that EGCG has anti-tumor, anti-oxidant, anti-inflammatory, and neuroprotective effects,²³ some of which involve activation of PKC isoforms.^{24,41} However, the mechanism remains obscure. In the present study, we are the first to report that EGCG is a new mild agonist of PKC α . First, we found that EGCG has the chemical affinity by allosterically binding to the catalytic C3–C4 domain of PKC α . Through the analysis of computational prediction AutoDock 4.2 software, we found EGCG could enter the active substrate-binding pocket on the catalytic C3–C4 domain of PKC α , which is the interaction bases between small molecule compound and protein.⁴² Thereafter, we identified that EGCG established

hydrogen bond polar interactions with V420, T401, E387, and K368 through the hydroxyl of phenol-OH, and the benzene ring group of EGCG hydrophobically binds to the hydrophobic pocket formed by L345, M470, I479, and V353 with the enhanced polar interaction through inserting the hydroxyl group into the hydrophobic pocket. Importantly, the allosteric interaction between EGCG and PKC α can be space-blocked by Ro-32-0432, a well-known PKC α agonist,^{43,44} because Ro-32-0432 also directly interacted with V420 of PKC α and the benzene ring group of Ro-32-0432 bound the same hydrophobic pocket of PKC α as EGCG. The SPR analysis implied that Ro-32-0432 can effectively block the affinity of EGCG to

PKC α . All these results implied that Ro-32-0432 could block the EGCG-induced activation of PKC α via a competitive mechanism. Comparing the binding confirmations of EGCG and Ro-32-0432 to PKC α , we found that the hydrogen bonds to T401, E387, and K368 were only observed during the binding of EGCG to PKC α . Therefore, we considered that these T401, E387, and K368 might be essential for the activation of PKC α by EGCG. However, which one or more of the predicted binding residuals is essential for the interaction between EGCG and PKC α still needs to be better understood with mutant PKC α . Besides, Ro-32-0432 displays about a 10-fold greater selectivity for PKC α ($IC_{50} = 9$ nM) and a 4-fold greater selectivity for PKC β I ($IC_{50} = 28$ nM) over PKC ϵ ($IC_{50} = 108$ nM).^{43,44} We here used 20 nmol/L Ro-32-0432 to selectively inhibit the activity of PKC α *in vitro* as previously directed.⁴⁵

Second, we demonstrated that EGCG has the bioactivity by acting on PKC α . In the present study, through *in vitro* cell culture and kinase activity assay, we found that EGCG could effectively activate PKC α indicated by dose-dependently triggered subcellular redistribution and dose-dependently increased activity of PKC α under the administration of 10^{-8} to 10^{-4} mol/L EGCG. Thereafter, to further evaluate the biological significance of EGCG on PKC α activation, we selected an animal model of long-term estrogen-deficient mice, which was previously demonstrated with downregulated PKC α and impaired cognitive function.³² Thus, we explored whether *in vivo* administration of EGCG could improve the cognition of OVX mice. The bioavailability of EGCG following oral intake is only 13.7%.⁴⁶ More precisely, about 3 ng/mg EGCG can enter the brain tissue following a 40 mg/kg EGCG administration by oral gavage.⁴⁷ Intraperitoneal injection can significantly elevate the bioavailability of drugs, but the pharmacokinetic properties of EGCG following intraperitoneal injection is still not clear. Rezai-Zadehet al. intraperitoneally injected 20 mg/kg EGCG to alleviate the brain A β deposition in Alzheimer's mice.⁴⁸ Therefore, we intraperitoneally injected 5, 10, and 20 mg/kg/day EGCG to OVX mice for 1 month, and observed improved cognitive function through the new object recognition task and Barnes maze, and rescued hippocampal synaptic plasticity through field potential recording. Furthermore, intraperitoneally co-injected Ro-32-0432 reverted the cognitive function and hippocampal LTP improved by EGCG. Bath application of Ro-32-0432 also reverted the improved LTP in all dose EGCG-treated OVX mice. Therefore, we conclude that EGCG improves the cognitive function and hippocampal synaptic plasticity of long-term estrogen-deficient mice through activating PKC α .

Collectively, in this work, EGCG was identified as a novel small-molecule PKC α agonist, which has a mild degree affinity to the catalytic C3–C4 domain of PKC α and good bioactivity both *in vivo* and *in vitro*. This finding encourages the clinical application of EGCG in cognitive impairment therapy. EGCG opens the way to a new perspective in PKC α biology and pharmacology. In particular, the elucidation of the structural requirements underlying its selectivity for PKC α will be crucial to the structure-based design of other PKC isozyme-selective agents. In turn, these new agents will help in the elucidation of the specific functions of PKC isozymes in human diseases. Altogether, EGCG will contribute to the redefinition of PKC α as feasible therapeutic targets in clinics.

MATERIALS AND METHODS

Animals. The 3 month old female C57BL/6 mice were housed under standard conditions (temperature 23 ± 1 °C; humidity 55–60%). Animals were maintained on a 12 h dark–light artificial cycle, with food and water ad libitum. OVX surgery was performed as previously described.⁴⁹ Briefly, mice were anesthetized with sodium pentobarbital (100 mg/kg, i.p.). After anesthesia, a dorsal incision was made and the ovary, oviduct, and top of the fallopian tubes were then clamped and removed. Five months after surgery, the mice were used for behavioral and electrophysiological experiments. All animal procedures were approved by the Institutional Animal Care and Use Committee at Harbin Medical University (no. HMUIRB-2008-06). All procedures were conformed to the Directive 2010/63/EU of the European Parliament.

Cell Cultures and Transfections. The hippocampal and cortical regions were removed from postnatal day 0 rat pups. After tissues were dissected and triturated, they were plated onto cell plates precoated with 10 μ g/mL poly-D-lysine (Sigma) and cultured in culture media containing neurobasal medium (Invitrogen) with 2% B27 supplement (Invitrogen) and 10% fetal bovine serum (HyClone). After 3 d, the neurons were treated with 5 μ M cytosine arabinoside (Sigma) to inhibit astrocyte proliferation. 5–7 d after plating, the neurons were transfected with GFP-fused-PKC α plasmid (Genechem) with Lipofectamine 2000 (Invitrogen) following the manufacturer's protocols. After 24 h of transfection, EGCG was freshly prepared and administrated to neurons.⁵⁰

Immunocytochemistry. After cell culture, transfection, and EGCG administration, cells were fixed with 4% paraformaldehyde + 4% sucrose for 15 min, and then, coverslips were washed 3× times 1× phosphate-buffered saline (PBS) and mounted with Fluoromount-G (SouthernBiotech; Birmingham, AL). Fluorescent images were acquired with a Zeiss LSM 800 confocal microscope (Carl Zeiss AG, Oberkochen, Germany). Cells were chosen from three or more independent cultures. Images were taken from at least three coverslips per experiment.

In Vitro PKC α Activity Assay. The nonradioactive PKC kinase activity kit (ADI-EKS-420A, Enzo Life Sciences) and purified recombinant human PKC α protein (Sigma, CAS 145333-02-4) were used. Briefly, 6 ng of PKC α was incubated with 10^{-8} to 10^{-4} M EGCG for 1 h and then transferred to a 96-well plate precoated with a peptide pseudosubstrates for 90 min at 37 °C. Subsequently, a phospho-specific substrate antibody that recognizes the phosphorylated form of the substrate was added and detected using a peroxidase-conjugated antibody. The degree of PKC activation was directly proportional to the amount of the phosphorylated substrate determined by measuring OD450 (BioTeck Synergy HT Spectrophotometer). EC₅₀ values were calculated considering the maximal response achieved by EGCG.

SPR Analysis. To examine the binding of EGCG to PKC α , SPR was performed on an OpenSPR system (Nicoya Lifesciences Inc., Kitchener, Canada) according to the previous description.⁵¹ The His-tagged protein PKC α was attached to COOH-sensor chips. Subsequently, EGCG solutions were introduced into the sensor chip with PBS as the running buffer. Finally, the kinetic constants, including the association constant (k_a), dissociation constant (k_d), and binding-affinity constant (K_D , $K_D = k_d/k_a$), were calculated using Trace Drawer software (Ridgeview Instruments AB, The Kingdom of Sweden) according to a 1:1 binding model.

Molecular Docking. The full-length amino acid sequence of PKC α is MADVFPGNSTASQDVANRFARKGALRKQNVHEVKDHKFIARFFKQPTFCSHCTDFIWFGFKQGFQCQVCCFVVHKRCHEFVTFSCKPAGDKGPDTDDPRSKHFKIHTYGSPTFC-DHCGSLLYGLIHQGMKCDTCDMNVKQCVINVPSLCGM-DHTEKRGRRIYLKAEVADEKLHVTVRDAKNLIPMDPNGLSD-PYVVLKLIPDPKNESKQKTIRSTLNQPNWESFTFKLK-PSDKDRRLSVEIWDWDRTRNDFMGSLSGVSELM-KMPASGWYKLLNQEEGEYYNVPIPEGDEEGNMELRQKFE-KAKLGPAGNKVISPSEDRKQPSNNLDRVKLDFNLFMLVLGK-GSFGKVMLADRKGTEELYAIKILKKDVTIQDDDVECTMVEKR-

VLALLDKPPLTQLHSCFQTVDRLYFVMEYVNGGDLMYHIQQ-VGKFKEPVAFYAAEISIGLFFLHKRGIIYRDLKLDNVMLDSE-GHIKIADFGMCKEHMMMDGVTRTFCGTPDYIAPEIIAY-QPYGKSVDWVAYGVLLYEMLAGQPPFDGEDEDELQSIMEH-NVSYPKSLSKAECVCKGLMTKHAKRLGCGPEGERDVRE-HAFFRIRDWEKLENREIQPPFKPKVCGKGKAENFDKFFTRGQ-PVLTPPDQLVIANIDQSDFEGFSYVNPQFVHPILQSAV. Accordingly, the crystallographic structure of PKC α with PDB codes 2ELI (C1 domain), 4DNL (C2 domain), and 4RA4 (catalytic C3–C4 domain) was used to test the binding mode of EGCG. First, the active pocket of the PKC α molecule was predicted with Pymol software. AutoDock 4.2 was then used to predict the binding conformations between EGCG and PKC α with a docking box centered on the active pocket. The binding conformations were ranked according to binding orientation, position, and energy. The binding conformation with the lowest energy was used for molecular dynamics analysis with AMBER16 software. After energy minimization and system equilibrium, the molecular dynamics were simulated and the root-mean-square deviation value was calculated.

Behavioral Test. Novel Object Recognition. Novel object recognition tests were done as previously described.^{52–54} Before the familiarization session, mice were allowed to freely move in the open field for habituation. One day after habituation, mice were allowed to freely explore two identical objects (Lego Bricks, 12.5 cm high, 2.5 cm deep, and 7.5 cm wide, built from blue, yellow, red, and green bricks) placed into the arena at fixed locations for 10 min. The SuperMaze video-tracking system (XinRuan, Shanghai, China), which is based on nose-point detection, was used to record the time spent exploring objects. Active exploration was defined as mice sniffing or touching the object when the gap between the nose and the object was less than 2 cm. At the end of the test, each mouse was returned to its home cage, and the chamber and objects were cleaned using 75% ethanol and then air-dried for 3 min. After an intersession interval of 24 h, one of the familiar objects was replaced by a novel object (tissue culture flasks, 15.5 cm high, 3.5 cm deep, and 9 cm wide, transparent plastic with a blue bottle cap). The location of the novel object (left or right) was randomized among the mice and the groups tested. Object preference was calculated by using the following formula: preference % = (time to explore the individual object/total exploration time for both objects) × 100%. Data were excluded if the total exploration duration was less than 10 s.

Barnes Maze. Barnes maze methods have been described previously.^{55,56} The Barnes maze consisted of an exposed and elevated, brightly lit circular white platform (91 cm in diameter) with 20 evenly spaced holes (5 cm in diameter) along the perimeter, one of which led to an escape port. Extra-maze cues consisted of specific symbols on the walls around the maze and the general layout of equipment in the room. The whole test consists of habituation, acquisition, and probe trials. During the habituation phase, mice were placed in the escape tunnel for 1 min. Also, mice were placed in the center of the apparatus to explore until entering the escape tunnel or 5 min elapses. The apparatus and tunnel were cleaned with 70% ethanol and air-dried for 3 min. Acquisition training (day 1 to day 5) consists of two acquisition trials daily (3 min limit per trial; intertrial interval ~1 h) with the starting location varied pseudorandomly among the four quadrants. At the start of each trial, the mouse is placed in a start chamber located in the center of one of the four quadrants. After 15 s, the start chamber is lifted and the mouse is allowed to explore the maze. During each trial, wind and bright light were played to induce escape behavior. The trial terminates when the mouse enters the escape tunnel or 3 min elapses. If a mouse fails to find the escape tunnel within the 3 min period, it will be placed in the tunnel by the researcher and allowed to stay there for 15 s before removal. Three days after the final session of acquisition training, mice undergo a 1 min probe trial (day 9) in which the escape tunnel is removed from the apparatus. The probe trial is administered similarly to the acquisition trials, except that the start chamber is placed in the center of the apparatus, rather than the center of any given quadrant. For each trial, the number of incorrect holes checked (error times) and

distance traveled (path length) before entering the tunnel are recorded to assess performance.

Electrophysiology. The hippocampal slices were prepared as previously reported.⁵⁷ Briefly, the mice were anesthetized with 20% urethane intraperitoneally and decapitated. Then, the hippocampus was carefully sliced (380 μ m thick) with Leica VT1200S microtome (Leica, Nussloch, Germany) in ice-cold dissection buffer [NMDG solution in mM: 93 NMDG, 2.5 KCl, 10 MgSO₄, 1.2 NaH₂PO₄, 30 NaHCO₃, 20 N-(2-hydroxyethyl)piperazine-N'-ethanesulfonic acid (HEPES), 0.5 CaCl₂, 25 d-glucose, 5 sodium-ascorbate, 3 sodium-pyruvate, 2 thiourea, and 2 N-acetyl-L-cysteine, with pH 7.3–7.4 adjusted by NaOH or HCl saturated with O₂ (95%)/CO₂ (5%) carbogen mixture]. The slices were then transferred into O₂ (95%)/CO₂ (5%)-saturated incubation solution containing (in mM): 124 NaCl, 2.5 KCl, 1.2 NaH₂PO₄, 24 NaHCO₃, 2 MgSO₄, 2 CaCl₂, 5 HEPES, 2 N-acetyl-L-cysteine, and 12.5 d-glucose (pH 7.3–7.4) for at least 1 h at 33 ± 2 °C. The recording slices were maintained in standard artificial cerebrospinal fluid solution (in mM: 124 NaCl, 2.5 KCl, 1.2 NaH₂PO₄, 24 NaHCO₃, 2 CaCl₂, 2 MgSO₄, 5 HEPES, and 10 d-glucose) at a constant flow (2–3 mL/min) and constant temperature of 33 ± 2 °C with the help of a temperature controller (TC-324C, Warner Instruments). During recording, a concentric bipolar microelectrode (CBARC75, FHC, USA) was placed in the Schaffer collateral (SC) domain with a 300 μ m distance away from recording pipettes in the stratum radiatum of the CA1 area. The recording pipettes were pulled from borosilicate glass (BF100-58-10, Sutter Instrument) with resistances of 2–3 MΩ when filled with a NaCl (3 mol/L) solution. Field excitatory postsynaptic potential (fEPSP) of SC-CA1 was evoked by a stimulatory isolator ISO-Flex (AMPI, Jerusalem, Israel) controlled by a Master-8 pulse generator (AMPI, Jerusalem, Israel). Analogue signals were bypass-filtered and digitized at 6 kHz using a Digidata 1550A and pClamp10 software (Molecular Devices, US). For each slice, an input–output response was tested, and the baseline fEPSP was set at ≈30% (for LTP experiments) of the maximal slope. Baseline stimulation was delivered every 30 s for at least 20 min before LTP induction to ensure the stability of the response. LTP was induced by using θ-burst stimulation (4 pulses at 100 Hz, with the bursts repeated at 5 Hz and each tetanus including three 10-burst trains separated by 15 s). Responses were recorded for 1 h after induction of LTP.⁵⁸ All electrophysiological data were collected with pCLAMP software (Molecular Devices) and analyzed blindly.

Drugs and Agents. EGCG was purchased from Sigma (catalog# E4143). 5, 10, and 20 mg/kg EGCG was intraperitoneally administrated to OVX mice for 1 month from 4 months after surgery. EGCG was freshly dissolved with saline before usage.

Statistical Analysis. Data are presented as the mean ± scanning electron microscopy (SEM) Statistical analyses were performed using Student's t-test for pairwise comparisons and one-way ANOVA with Tukey post hoc tests for comparisons of more than two groups. All statistical analyses were performed using SAS 9.1 software (serial number: 989155; SAS Institute Inc., Cary, NC, USA). Significance was accepted at $P < 0.05$, and graphs were generated using GraphPad Prism 5.0 software (La Jolla, CA, USA).

ASSOCIATED CONTENT

Supporting Information

The Supporting Information is available free of charge at <https://pubs.acs.org/doi/10.1021/acschemneuro.1c00401>.

Additional PKC α structures, docking data, and behavioral results ([PDF](#))

AUTHOR INFORMATION

Corresponding Author

Jing Ai – Department of Pharmacology (The State-Province Key Laboratories of Biomedicine-Pharmaceutics of China), College of Pharmacy of Harbin Medical University, Harbin,

Heilongjiang Province 150086, China; orcid.org/0000-0001-6496-7059; Phone: +86 451 86671354;
Email: azhrbmu@126.com, aijing@ems.hrbmu.edu.cn;
Fax: +86 451 86671354

Authors

- Shuai Zhang** – Department of Pharmacology (The State-Province Key Laboratories of Biomedicine-Pharmaceutics of China), College of Pharmacy of Harbin Medical University, Harbin, Heilongjiang Province 150086, China
- Yi Xu** – Department of Pharmacology (The State-Province Key Laboratories of Biomedicine-Pharmaceutics of China), College of Pharmacy of Harbin Medical University, Harbin, Heilongjiang Province 150086, China
- Lu Zeng** – Department of Pharmacology (The State-Province Key Laboratories of Biomedicine-Pharmaceutics of China), College of Pharmacy of Harbin Medical University, Harbin, Heilongjiang Province 150086, China
- Xiaobin An** – Department of Pharmacology (The State-Province Key Laboratories of Biomedicine-Pharmaceutics of China), College of Pharmacy of Harbin Medical University, Harbin, Heilongjiang Province 150086, China
- Dan Su** – Department of Pharmacology (The State-Province Key Laboratories of Biomedicine-Pharmaceutics of China), College of Pharmacy of Harbin Medical University, Harbin, Heilongjiang Province 150086, China
- Yang Qu** – Department of Pharmacology (The State-Province Key Laboratories of Biomedicine-Pharmaceutics of China), College of Pharmacy of Harbin Medical University, Harbin, Heilongjiang Province 150086, China
- Jing Ma** – Department of Pharmacology (The State-Province Key Laboratories of Biomedicine-Pharmaceutics of China), College of Pharmacy of Harbin Medical University, Harbin, Heilongjiang Province 150086, China
- Xin Tang** – Department of Pharmacology (The State-Province Key Laboratories of Biomedicine-Pharmaceutics of China), College of Pharmacy of Harbin Medical University, Harbin, Heilongjiang Province 150086, China
- Xuqiao Wang** – Department of Pharmacology (The State-Province Key Laboratories of Biomedicine-Pharmaceutics of China), College of Pharmacy of Harbin Medical University, Harbin, Heilongjiang Province 150086, China
- Junkai Yang** – Department of Pharmacology (The State-Province Key Laboratories of Biomedicine-Pharmaceutics of China), College of Pharmacy of Harbin Medical University, Harbin, Heilongjiang Province 150086, China
- Chandan Mishra** – Department of Pharmacology (The State-Province Key Laboratories of Biomedicine-Pharmaceutics of China), College of Pharmacy of Harbin Medical University, Harbin, Heilongjiang Province 150086, China
- Shah Ram Chandra** – Department of Pharmacology (The State-Province Key Laboratories of Biomedicine-Pharmaceutics of China), College of Pharmacy of Harbin Medical University, Harbin, Heilongjiang Province 150086, China

Complete contact information is available at:
<https://pubs.acs.org/10.1021/acschemneuro.1c00401>

Author Contributions

S.Z. and Y.X. contributed equally to this work. The manuscript was written through contributions of all authors. All authors have given approval to the final version of the manuscript.

Notes

The authors declare no competing financial interest.

ACKNOWLEDGMENTS

This work was supported by the National Natural Science Foundation of China (81870849 and 81671052 to J.A.), Natural Science Foundation of Heilongjiang province (ZD2018004 to J.A.), and Heilongjiang Touyan Innovation Team Program.

REFERENCES

- (1) Mackay, H. J.; Twelves, C. J. Targeting the protein kinase C family: are we there yet? *Nat. Rev. Canc.* **2007**, *7*, 554–562.
- (2) Sun, M.-K.; Alkon, D. L. The "memory kinases": roles of PKC isoforms in signal processing and memory formation. *Prog. Mol. Biol. Transl. Sci.* **2014**, *122*, 31–59.
- (3) Braz, J. C.; Gregory, K.; Pathak, A.; Zhao, W.; Sahin, B.; Klevitsky, R.; Kimball, T. F.; Lorenz, J. N.; Baird, A. C.; Liggett, S. B.; Boden, I.; Wang, S.; Schwartz, A.; Lakatta, E. G.; DePaoli-Roach, A. A.; Robbins, J.; Hewett, T. E.; Bibb, J. A.; Westfall, M. V.; Kranias, E. G.; Molkentin, J. D. PKC-alpha regulates cardiac contractility and propensity toward heart failure. *Nat. Med.* **2004**, *10*, 248.
- (4) Geraldes, P.; King, G. L. Activation of protein kinase C isoforms and its impact on diabetic complications. *Circ. Res.* **2010**, *106*, 1319–1331.
- (5) Isakov, N. Protein kinase C (PKC) isoforms in cancer, tumor promotion and tumor suppression. *Semin. Canc. Biol.* **2018**, *48*, 36–52.
- (6) Alkon, D. L.; Sun, M.-K.; Nelson, T. J. PKC signaling deficits: a mechanistic hypothesis for the origins of Alzheimer's disease. *Trends Pharmacol. Sci.* **2007**, *28*, 51–60.
- (7) Mochly-Rosen, D.; Das, K.; Grimes, K. V. Protein kinase C, an elusive therapeutic target? *Nat. Rev. Drug Discov.* **2012**, *11*, 937–957.
- (8) Ohno, S.; Kawasaki, H.; Imajoh, S.; Suzuki, K.; Inagaki, M.; Yokokura, H.; Sakoh, T.; Hidaka, H. Tissue-specific expression of three distinct types of rabbit protein kinase C. *Nature* **1987**, *325*, 161–166.
- (9) Partovian, C.; Zhuang, Z.; Moodie, K.; Lin, M.; Ouchi, N.; Sessa, W. C.; Walsh, K.; Simons, M. PKC α activates eNOS and increases arterial blood flow in vivo. *Circ. Res.* **2005**, *97*, 482.
- (10) Wynne, B. M.; McCarthy, C. G.; Szasz, T.; Molina, P. A.; Chapman, A. B.; Webb, R. C.; Klein, J. D.; Hoover, R. S. Protein kinase C α deletion causes hypotension and decreased vascular contractility. *J. Hypertens.* **2018**, *36*, 510–519.
- (11) Nowak, G.; Bakajsova, D. Protein kinase C- α activation promotes recovery of mitochondrial function and cell survival following oxidant injury in renal cells. *Am. J. Physiol. Ren. Physiol.* **2012**, *303*, F515–F526.
- (12) Hongpaisan, J.; Xu, C.; Sen, A.; Nelson, T. J.; Alkon, D. L. PKC activation during training restores mushroom spine synapses and memory in the aged rat. *Neurobiol. Dis.* **2013**, *55*, 44–62.
- (13) Etchebeheregaray, R.; Tan, M.; Dewachter, I.; Kuiper, C.; Van der Auwera, I.; Wera, S.; Qiao, L.; Bank, B.; Nelson, T. J.; Kozikowski, A. P.; Van Leuven, F.; Alkon, D. L. Therapeutic effects of PKC activators in Alzheimer's disease transgenic mice. *Proc. Natl. Acad. Sci. U.S.A.* **2004**, *101*, 11141–11146.
- (14) Nelson, T. J.; Alkon, D. L. Neuroprotective versus tumorigenic protein kinase C activators. *Trends Biochem. Sci.* **2009**, *34*, 136–145.
- (15) Wender, P. A.; Cribbs, C. M.; Koehler, K. F.; Sharkey, N. A.; Herald, C. L.; Kamano, Y.; Pettit, G. R.; Blumberg, P. M. Modeling of the bryostatins to the phorbol ester pharmacophore on protein kinase C. *Proc. Natl. Acad. Sci. U.S.A.* **1988**, *85*, 7197–7201.
- (16) Jeffrey, A. M.; Liskamp, R. M. Computer-assisted molecular modeling of tumor promoters: rationale for the activity of phorbol esters, teleocidin B, and aplysia toxin. *Proc. Natl. Acad. Sci. U.S.A.* **1986**, *83*, 241–245.

- (17) Zhang, G.; Kazanietz, M. G.; Blumberg, P. M.; Hurley, J. H. Crystal structure of the cys2 activator-binding domain of protein kinase C delta in complex with phorbol ester. *Cell* **1995**, *81*, 917–924.
- (18) Ajani, J. A.; Jiang, Y.; Faust, J.; Chang, B. B.; Ho, L.; Yao, J. C.; Rousey, S.; Dakhil, S.; Cherny, R. C.; Craig, C.; Bleyer, A. A multicenter phase II study of sequential paclitaxel and bryostatin-1 (NSC 339555) in patients with untreated, advanced gastric or gastroesophageal junction adenocarcinoma. *Invest. New Drugs* **2006**, *24*, 353–357.
- (19) Ku, G. Y.; Ilson, D. H.; Schwartz, L. H.; Capanu, M.; O'Reilly, E.; Shah, M. A.; Kelsen, D. P.; Schwartz, G. K. Phase II trial of sequential paclitaxel and 1 h infusion of bryostatin-1 in patients with advanced esophageal cancer. *Canc. Chemother. Pharmacol.* **2008**, *62*, 875–880.
- (20) Griner, E. M.; Kazanietz, M. G. Protein kinase C and other diacylglycerol effectors in cancer. *Nat. Rev. Canc.* **2007**, *7*, 281–294.
- (21) Lambert, J. D.; Sang, S.; Yang, C. S. Possible controversy over dietary polyphenols: benefits vs risks. *Chem. Res. Toxicol.* **2007**, *20*, 583–585.
- (22) Steinmann, J.; Buer, J.; Pietschmann, T.; Steinmann, E. Anti-infective properties of epigallocatechin-3-gallate (EGCG), a component of green tea. *Br. J. Pharmacol.* **2013**, *168*, 1059–1073.
- (23) Yang, C. S.; Wang, X.; Lu, G.; Picinich, S. C. Cancer prevention by tea: animal studies, molecular mechanisms and human relevance. *Nat. Rev. Canc.* **2009**, *9*, 429–439.
- (24) Zhao, X.; Liu, F.; Jin, H.; Li, R.; Wang, Y.; Zhang, W.; Wang, H.; Chen, W. Involvement of PKC α and ERK1/2 signaling pathways in EGCG's protection against stress-induced neural injuries in Wistar rats. *Neuroscience* **2017**, *346*, 226–237.
- (25) Ahmed, R.; VanSchouwen, B.; Jafari, N.; Ni, X.; Ortega, J.; Melacini, G. Molecular Mechanism for the (-)-Epigallocatechin Gallate-Induced Toxic to Nontoxic Remodeling of A β Oligomers. *J. Am. Chem. Soc.* **2017**, *139*, 13720–13734.
- (26) Gundimeda, U.; McNeill, T. H.; Elhiani, A. A.; Schiffman, J. E.; Hinton, D. R.; Gopalakrishna, R. Green tea polyphenols precondition against cell death induced by oxygen-glucose deprivation via stimulation of laminin receptor, generation of reactive oxygen species, and activation of protein kinase C epsilon. *J. Biol. Chem.* **2012**, *287*, 34694–34708.
- (27) Chou, C.-W.; Huang, W.-J.; Tien, L.-T.; Wang, S.-J. (-)-Epigallocatechin gallate, the most active polyphenolic catechin in green tea, presynaptically facilitates Ca $^{2+}$ -dependent glutamate release via activation of protein kinase C in rat cerebral cortex. *Synapse* **2007**, *61*, 889–902.
- (28) Mochly-Rosen, D. Localization of protein kinases by anchoring proteins: a theme in signal transduction. *Science* **1995**, *268*, 247–251.
- (29) Bessa, C.; Soares, J.; Raimundo, L.; Loureiro, J. B.; Gomes, C.; Reis, F.; Soares, M. L.; Santos, D.; Dureja, C.; Chaudhuri, S. R.; Lopez-Haber, C.; Kazanietz, M. G.; Gonçalves, J.; Simões, M. F.; Rijo, P.; Saraiva, L. Discovery of a small-molecule protein kinase C δ -selective activator with promising application in colon cancer therapy. *Cell Death Dis.* **2018**, *9*, 23.
- (30) Ito, A.; Saito, N.; Hirata, M.; Kose, A.; Tsujino, T.; Yoshihara, C.; Ogita, K.; Kishimoto, A.; Nishizuka, Y.; Tanaka, C. Immunocytochemical localization of the alpha subspecies of protein kinase C in rat brain. *Proc. Natl. Acad. Sci. U.S.A.* **1990**, *87*, 3195–3199.
- (31) Colgan, L. A.; Hu, M.; Misler, J. A.; Parra-Bueno, P.; Moran, C. M.; Leitges, M.; Yasuda, R. PKC α integrates spatiotemporally distinct Ca and autocrine BDNF signaling to facilitate synaptic plasticity. *Nat. Neurosci.* **2018**, *21*, 1027.
- (32) Zhang, S.; An, X.-B.; Huang, S.-Y.; Zeng, L.; Xu, Y.; Su, D.; Qu, Y.; Tang, X.; Ma, J.; Yang, J.-K.; Ai, J. AhR/miR-23a-3p/PKC α axis contributes to memory deficits in ovariectomized and normal aging female mice. *Mol. Ther.-Nucleic Acids* **2021**, *24*, 79–91.
- (33) Kvirvelia, N.; McMenamin, M.; Warren, M.; Jadeja, R. N.; Kodeboyna, S. K.; Sharma, A.; Zhi, W.; O'Connor, P. M.; Raju, R.; Lucas, R.; Madaio, M. P. Kidney-targeted inhibition of protein kinase C α ameliorates nephrotoxic nephritis with restoration of mitochondrial dysfunction. *Kidney Int.* **2018**, *94*, 280–291.
- (34) Zhao, X.; Liu, F.; Jin, H.; Li, R.; Wang, Y.; Zhang, W.; Wang, H.; Chen, W. Involvement of PKC α and ERK1/2 signaling pathways in EGCG's protection against stress-induced neural injuries in Wistar rats. *Neuroscience* **2017**, *346*, 226–237.
- (35) Lynch, M. A. Long-term potentiation and memory. *Physiol. Rev.* **2004**, *84*, 87–136.
- (36) Dupasquier, S.; Blache, P.; Picque Lasorsa, L.; Zhao, H.; Abraham, J. D.; Haigh, J. J.; Ychou, M.; Prévostel, C. Modulating PKC α Activity to Target Wnt/ β -Catenin Signaling in Colon Cancer. *Cancers* **2019**, *11*, 693.
- (37) Tsai, J. H.; Hsieh, Y. S.; Kuo, S. J.; Chen, S. T.; Yu, S. Y.; Huang, C. Y.; Chang, A. C.; Wang, Y. W.; Tsai, M. T.; Liu, J. Y. Alteration in the expression of protein kinase C isoforms in human hepatocellular carcinoma. *Canc. Lett.* **2000**, *161*, 171–175.
- (38) Hudson, B. D.; Hidalgo, C. G.; Gotthardt, M.; Granzier, H. L. Excision of titin's cardiac PEVK spring element abolishes PKC α -induced increases in myocardial stiffness. *J. Mol. Cell. Cardiol.* **2010**, *48*, 972–978.
- (39) Hongpaisan, J.; Alkon, D. L. A structural basis for enhancement of long-term associative memory in single dendritic spines regulated by PKC. *Proc. Natl. Acad. Sci. U.S.A.* **2007**, *104*, 19571–19576.
- (40) Cascella, M.; Bimonte, S.; Muzio, M. R.; Schiavone, V.; Cuomo, A. The efficacy of Epigallocatechin-3-gallate (green tea) in the treatment of Alzheimer's disease: an overview of pre-clinical studies and translational perspectives in clinical practice. *Infect. Agents Canc.* **2017**, *12*, 36.
- (41) Menard, C.; Bastianetto, S.; Quirion, R. Neuroprotective effects of resveratrol and epigallocatechin gallate polyphenols are mediated by the activation of protein kinase C gamma. *Front. Cell. Neurosci.* **2013**, *7*, 281.
- (42) George, D. M.; Breinlinger, E. C.; Argiriadi, M. A.; Zhang, Y.; Wang, J.; Bansal-Pakala, P.; Duignan, D. B.; Honore, P.; Lang, Q.; Mittelstadt, S.; Rundell, L.; Schwartz, A.; Sun, J.; Edmunds, J. J. Optimized protein kinase C θ (PKC θ) inhibitors reveal only modest anti-inflammatory efficacy in a rodent model of arthritis. *J. Med. Chem.* **2015**, *58*, 333–346.
- (43) Wilkinson, S. E.; Parker, P. J.; Nixon, J. S. Isoenzyme specificity of bisindolylmaleimides, selective inhibitors of protein kinase C. *Biochem. J.* **1993**, *294*, 335–337.
- (44) Birchall, A. M.; Bishop, J.; Bradshaw, D.; Cline, A.; Coffey, J.; Elliott, L. H.; Gibson, V. M.; Greenham, A.; Hallam, T. J.; Harris, W. Ro 32-0432, a selective and orally active inhibitor of protein kinase C prevents T-cell activation. *J. Pharmacol. Exp. Therapeut.* **1994**, *268*, 922–929.
- (45) Kim, H.; Han, S. H.; Quan, H. Y.; Jung, Y.-J.; An, J.; Kang, P.; Park, J.-B.; Yoon, B.-J.; Seol, G. H.; Min, S. S. Bryostatin-1 promotes long-term potentiation via activation of PKC α and PKC ϵ in the hippocampus. *Neuroscience* **2012**, *226*, 348–355.
- (46) Yang, C. S.; Chen, L.; Lee, M. J.; Valentine, D.; Kuo, M. C.; Schantz, S. P. Blood and urine levels of tea catechins after ingestion of different amounts of green tea by human volunteers. *Cancer Epidemiol. Biomark. Prev.* **1998**, *7*, 351–354.
- (47) Ettcheto, M.; Cano, A.; Manzine, P. R.; Busquets, O.; Verdaguer, E.; Castro-Torres, R. D.; García, M. L.; Beas-Zarate, C.; Olloquequi, J.; Auladell, C.; Folch, J.; Camins, A. Epigallocatechin-3-Gallate (EGCG) Improves Cognitive Deficits Aggravated by an Obesogenic Diet Through Modulation of Unfolded Protein Response in APPswe/PS1dE9 Mice. *Mol. Neurobiol.* **2020**, *57*, 1814–1827.
- (48) Rezai-Zadeh, K.; Shytie, D.; Sun, N.; Mori, T.; Hou, H.; Jeanniton, D.; Ehrhart, J.; Townsend, K.; Zeng, J.; Morgan, D.; Hardy, J.; Town, T.; Tan, J. Green tea epigallocatechin-3-gallate (EGCG) modulates amyloid precursor protein cleavage and reduces cerebral amyloidosis in Alzheimer transgenic mice. *J. Neurosci.* **2005**, *25*, 8807–8814.
- (49) Sun, L.-Y.; Wang, N.; Ban, T.; Sun, Y.-H.; Han, Y.; Sun, L.-L.; Yan, Y.; Kang, X.-H.; Chen, S.; Sun, L.-H.; Zhang, R.; Zhao, Y.-J.; Zhang, H.; Ai, J.; Yang, B.-F. MicroRNA-23a mediates mitochondrial compromise in estrogen deficiency-induced concentric remodeling via targeting PGC-1 α . *J. Mol. Cell. Cardiol.* **2014**, *75*, 1–11.

- (50) Ai, J.; Sun, L.-H.; Che, H.; Zhang, R.; Zhang, T.-Z.; Wu, W.-C.; Su, X.-L.; Chen, X.; Yang, G.; Li, K.; Wang, N.; Ban, T.; Bao, Y.-N.; Guo, F.; Niu, H.-F.; Zhu, Y.-L.; Zhu, X.-Y.; Zhao, S.-G.; Yang, B.-F. MicroRNA-195 protects against dementia induced by chronic brain hypoperfusion via its anti-amyloidogenic effect in rats. *J. Neurosci.* **2013**, *33*, 3989–4001.
- (51) Zhang, H.; Zhao, Y.; Yu, M.; Zhao, Z.; Liu, P.; Cheng, H.; Ji, Y.; Jin, Y.; Sun, B.; Zhou, J.; Ding, Y. Reassembly of native components with donepezil to execute dual-missions in Alzheimer's disease therapy. *J. Contr. Release* **2019**, *296*, 14–28.
- (52) Tanila, H.; Sipilä, P.; Shapiro, M.; Eichenbaum, H. Brain aging: impaired coding of novel environmental cues. *J. Neurosci.* **1997**, *17*, 5167–5174.
- (53) Zhu, H.; Wang, N.; Yao, L.; Chen, Q.; Zhang, R.; Qian, J.; Hou, Y.; Guo, W.; Fan, S.; Liu, S.; Zhao, Q.; Du, F.; Zuo, X.; Guo, Y.; Xu, Y.; Li, J.; Xue, T.; Zhong, K.; Song, X.; Huang, G.; Xiong, W. Moderate UV Exposure Enhances Learning and Memory by Promoting a Novel Glutamate Biosynthetic Pathway in the Brain. *Cell* **2018**, *173*, 1716–1727.
- (54) Leger, M.; Quiedeville, A.; Bouet, V.; Haelewyn, B.; Boulouard, M.; Schumann-Bard, P.; Freret, T. Object recognition test in mice. *Nat. Protoc.* **2013**, *8*, 2531–2537.
- (55) Wahlstrom, K. L.; Huff, M. L.; Emmons, E. B.; Freeman, J. H.; Narayanan, N. S.; McIntyre, C. K.; LaLumiere, R. T. Basolateral Amygdala Inputs to the Medial Entorhinal Cortex Selectively Modulate the Consolidation of Spatial and Contextual Learning. *J. Neurosci.* **2018**, *38*, 2698–2712.
- (56) Pitts, M. W. Barnes Maze Procedure for Spatial Learning and Memory in Mice. *Bio Protoc.* **2018**, *8*, No. e2744.
- (57) Zhang, S.; Yan, M.-L.; Yang, L.; An, X.-B.; Zhao, H.-M.; Xia, S.-N.; Jin, Z.; Huang, S.-Y.; Qu, Y.; Ai, J. MicroRNA-153 impairs hippocampal synaptic vesicle trafficking via downregulation of synapsin I in rats following chronic cerebral hypoperfusion. *Exp. Neurol.* **2020**, *332*, 113389.
- (58) Knafo, S.; Sánchez-Puelles, C.; Palomer, E.; Delgado, I.; Draffin, J. E.; Mingo, J.; Wahle, T.; Kaleka, K.; Mou, L.; Pereda-Perez, I.; Klosi, E.; Faber, E. B.; Chapman, H. M.; Lozano-Montes, L.; Ortega-Molina, A.; Ordóñez-Gutiérrez, L.; Wandosell, F.; Viña, J.; Dotti, C. G.; Hall, R. A.; Pulido, R.; Gerges, N. Z.; Chan, A. M.; Spaller, M. R.; Serrano, M.; Venero, C.; Esteban, J. A. PTEN recruitment controls synaptic and cognitive function in Alzheimer's models. *Nat. Neurosci.* **2016**, *19*, 443–453.